DOUGLAS PAPER NO. 3525

COMPUTATIONAL METHODS FOR SPACE RADIATION SHIELDING ANALYSIS

M.P. BILLINGS
NUCLEAR ENGINEERING BRANCH
NUCLEAR DEPARTMENT-RESEARCH AND DEVELOPMENT
MISSILE AND SPACE SYSTEMS DIVISION
DOUGLAS AIRCRAFT COMPNAY INC

R.W. LANGLEY
CHIEF, NUCLEAR VEHICLE SUBSYSTEMS SECTION
NUCLEAR ENGINEERING BRANCH
NUCLEAR DEPARTMENT RESEARCH AND DEVELOPMENT
MISSILE AND SPACE SYSTEMS DIVISION
DOUGLAS AIRCRAFT COMPANY INC

DOUGLAS MISSILE & SPACE SYSTEMS DIVISION

ABSTRACT

Analytical methods and computer programs have been developed at Douglas for use in establishing the radiation shielding requirements of space vehicle systems. Current techniques for performing space radiation shielding analyses are reviewed in the context of the digital computer programs in which they have been incorporated. Calculations dealing with the transport of primary charged particles and secondary reaction products through matter are performed by the CHARGE program for geometrically simple systems. The calculation of radiation levels in geometrically complex vehicle-shield configurations is accomplished by the SIGMA program, using the QUAD generalized quadratic surface geometry package. Procedures for ascertaining the optimal distribution of shield mass subject to specific dose design criteria are presently under development.

1.0 INTRODUCTION

Since the mass of a space vehicle shielding system typically represents a considerable payload investment, an accurate assessment of shielding requirements is essential. The overestimation of shielding requirements can lead to an excessive weight burden, resulting in reduced vehicle performance margins, increased program costs, and a delay in space exploration. Conversely, the underestimation of shielding requirements can seriously jeopardize mission success.

Studies of space vehicle systems have shown that the establishment of a shield design effectively meeting the vehicle and mission requirements is a complex process. Most of the significant factors in space vehicle shielding analyses, i.e., the extant space radiation environment, the radiation level design criteria, the shield system geometric framework, etc., are sensitive functions of vehicle and mission characteristics. The nature of these relationships is indicated in the following:

1) The mission profile governs the relative importance of naturally occurring earth radiation belts, artificial belts, solar radiation, and galactic cosmic radiation; the dominant influences are due to the vehicle trajectory, the mission duration, and the time period of the mission with respect to the solar cycle.
2) Additional influences are due to those mission requirements affecting the size and shape of the crew compartment within which tolerable radiation levels are to be maintained, and the biomedical dose tolerances established for crew members.
3) The vehicle configuration is important since the internal arrangement of work and rest areas controls the time-dependent position of

crew members; the location of fixed equipment, structure, stores, etc., with respect to work stations and rest areas governs their effectiveness as shielding materials.

4) Both mission and vehicle characteristics influence the feasibility of, and benefits from, optimization of the shield design by distributing shield mass among such locations as crew compartment wall structure, biowells, localized shields and portable personal shields.

As a designer and manufacturer of space vehicle systems, Douglas has actively pursued the development of the shielding technology required to integrate vehicle and mission characteristics into shield system design. The shielding methodology thus developed has largely been incorporated in digital computer programs to facilitate its application to radiation protection design problems of realistic space vehicle systems. These design methods are reviewed here.

Emphasis is placed on the shielding technology related to the space radiation environment, rather than the neutron and gamma environments from on-board nuclear power systems. Douglas space radiation shielding technology is discussed in two major areas: shielding physics and applied shielding. The shielding physics efforts have concentrated on the mathematical formulation of the transport of radiation through matter, usually for simple geometric systems. Applied shielding has dealt with the calculation of radiation levels in specific source-vehicle-shield configurations, with the associated problems in treatment of geometric parameters and shield system optimization.

2.0 SPACE RADIATION SHIELDING ANALYSIS

Figure 1 illustrates the interrelationship of several computer programs currently utilized for space radiation shielding analyses. The manner in which a shielding optimization program now under development will be integrated with existing programs is also indicated.

Typically, the radiation analyses requisite to space vehicle design begin with the definition of the extant space environment in space, energy, and time. The space radiation sources which are important to space systems are magnetically trapped radiation, solar flares, and galactic cosmic rays. A computer program, OGRE, which Douglas has developed for describing geomagnetically trapped radiation, presently incorporates the latest available data on each of these sources and is capable of determining the space and time dependent and mission-integrated radiation which a space vehicle will encounter on a specified trajectory. A complete description of the data and analytical techniques used in the OGRE program is given in Reference 1.

Once the radiation environment has been defined, computations to establish radiation levels can be performed, the calculational problems becoming increasingly difficult as the geometry of the vehicle-shield system becomes more complex and the radiation fields become more extreme. The Douglas-developed CHARGE program is the primary calculational tool for ascertaining basic dose attenuation in simple geometries. CHARGE output data identifies critical organ dose due to each radiation source, i.e., trapped protons, trapped electrons, solar flare protons, secondary electron-bremsstrahlung, and secondary nucleons from proton interactions with the system materials.

INTERRELATIONSHIP OF SPACE RADIATION SHIELDING PROGRAMS

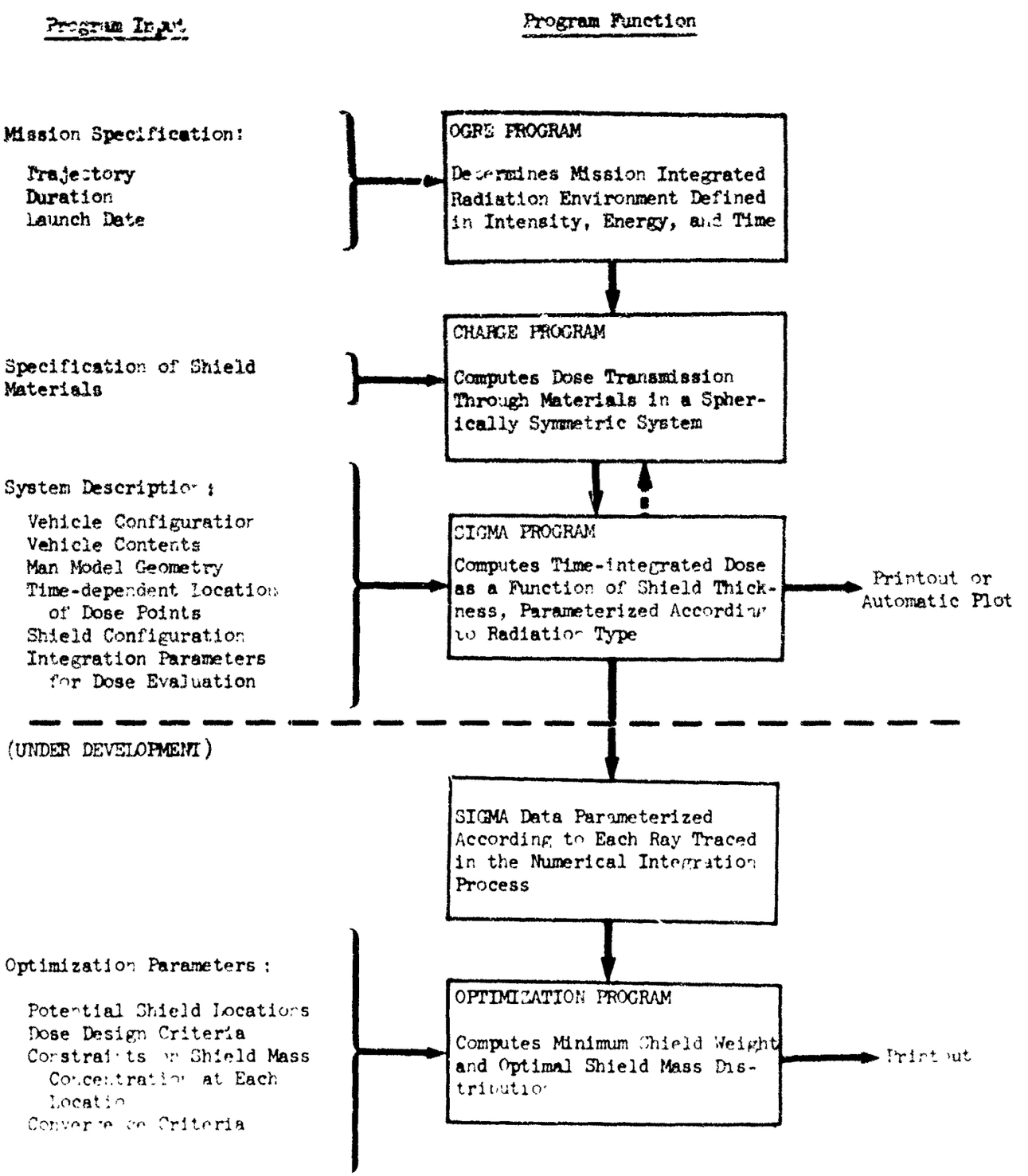

FIGURE 1

The Douglas-developed SIGMA program is used to perform dose calculations for realistic, geometrically complex space vehicle systems. This program incorporates a generalized quadratic surface geometry package by means of which the space vehicle is defined and ray tracing operations are performed. SIGMA computes the biological dose at specified receptor locations by performing a numerical integration of angularly dependent dose attenuation kernels over solid angle. The dose attenuation kernels necessary for this analysis are customarily constructed by curve-fitting basic CHARGE dose data; they are then evaluated within SIGMA, for the computed material distribution along each ray traced in the angular integration process, to obtain the dose contribution for each element of solid angle.

As an option, the dose contribution associated with each ray can be determined by performing a complete CHARGE radiation transport calculation for that particular material distribution. This capability is illustrated schematically in Figure 1 by the dotted arrow between the SIGMA and CHARGE programs blocks.

The existing OGRE, CHARGE, and SIGMA programs will be supplemented by a shield optimization program currently under development. This program will permit calculation of the minimum shield weight meeting specified dose design criteria. For this purpose, the parametric dependence of dose on the amount and disposition of the shield materials will be established by computations largely performed with existing programs. These parametric data will then be operated on by an iterative technique, based on the Lagrange method of undetermined multipliers, to determine the optimal distribution of shield material among several candidate locations identified as program input.

3.0 SHIELDING PHYSICS

A review of the CHARGE method of computing the transport of space radiations through matter is given in this section, together with comparisons of CHARGE results with experimental measurements and with data from independent analyses. Related work aimed at improving the mathematical models and basic nuclear data now incorporated in the CHARGE program is also presented.

3.1 The CHARGE Program

Shielding program CHARGE (Reference 2) provides a straight-ahead approximation solution to the radiation penetration problem for primary electrons with their associated bremsstrahlung, and primary protons with their associated secondary protons and neutrons, for geometrically simple shields. Proton and electron analyses use a modification of the range-energy relations applied to as many as one hundred energy groups. Secondary electron-bremsstrahlung transmission is based on exponential attenuation, using energy dependent non-elastic cross sections above 20 Mev and energy independent "removal" cross sections below 20 Mev.

CHARGE computes the dose rates and energy fluxes as a function of penetration into the shield. The calculation may optionally be halted before the entire shield is traversed by specifying a minimum total dose rate of interest, in which case it proceeds through a number of shield lamina just sufficient to reduce the dose rate below this value.

3.1.1 Primary Particle Calculations

The attenuation of primary charged particles is governed primarily by ionization of the shield materials. The primary radiation dose rates, D_γ, are computed by

numerical evaluation of the integral

$$\dot{D}_p(x) = C \int_{E_\ell(x)}^{E_h} \phi(E) \exp\left[-\int_0^x \sum_{ne}\left(E'(E,x')\right) dx'\right] \frac{d}{dx} E'(E,x) dE$$

where $E'(E,x)$ is the degraded energy at shield depth x (cm) corresponding to the incident energy E, and is calculated from the range-energy relation, (Mev)

C is the flux to dose rate conversion factor, (rad/hr)/(Mev/cm^3-sec)

$\phi(E)$ is the incident inward directed primary particle flux, (particles/Mev-cm^2-sec)

$\sum_{ne}(E')$ is the macroscopic cross section for non-elastic collisions, (cm^{-1})

E_h is the maximum energy of the incident particles, (Mev)

$E_\ell(x)$ is the energy which has range x in the shield material, (Mev).

The incident spectrum is divided into energy groups and the shield materials into layers for the penetration analysis. In contrast to usual multi-group treatments, the spectrum shape is retained within each energy group when performing the dose integral. This approach yields much more accurate results than is possible using many times the number of energy groups with a constant spectrum. Since the mean free path for non-elastic collisions is large compared to usual shield thicknesses, and varies little over wide ranges of energy, the integral in the nuclear attenuation term is closely approximated by a summation using average group energies. The incident group of charged particles is attenuated through the shield by an integration of $\frac{d}{dx} E'(E,x)$, determining the group boundary energies as a function of x. The treatment of electrons and protons differs slightly because of their different range-energy characteristics.

Charged Particle Spectra - The ambient electron and/or proton spectra may be specified as differential spectra in tabular or functional form. The energy dependence of these spectra is almost unlimited, and the energy ranges considered are limited only by the computer capabilities. These incident charged particle spectra, which may be viewed as essentially continuous functions of particle kinetic energy, are divided into energy bands or groups, the number (≤ 100) and spacing of which are controlled by input data. Each of these groups may be completely described by its upper and lower energy limits and the energy variation of the spectrum within the group, with CHARGE ensuring that the spectrum within any group is a single, continuous function of the energy.

Functional forms allowed for the ambient differential spectra include (1) a power law or (2) an exponential dependence; the spectrum may be specified for each of several energy ranges. Input data for either analytic form may consist of:

1) Total ambient particle densities.
2) Power of E or multiplier of E in exponent over each energy range (used for interpolation to energies not given in input).
3) Values of differential spectrum at input-specified energies.
4) Constants which multiply the power or exponent of E to give the density at each energy.

Proton Energy Loss Rates - The proton range-energy computation is based on the relativistic energy loss rate for "heavy" particles traversing a material and losing energy by ionization (i.e., elastic collision with atomic electrons). This formula, given in many references (e.g., Reference 3), is

$$-\frac{dE}{dx} = \frac{4\pi e^4 z^2}{mv^2} NB$$

where e is the electronic charge,

m is the electronic mass,

Z is the charge of the incident particle, units of e

v is the velocity of the incident particle,

N is the density of stopping atoms, and

B is the "stopping number".

According to the Bethe-Bloch theory

$$B = Z\left[\ln\left(\frac{2mv^2}{I}\right) - \ln(1-\beta^2) - \beta^2 - \delta\right]$$

where Z is the atomic number of the stopping material, I is the average ionization potential (energy to remove one electron) for the stopping atoms, β is v divided by c, the velocity of light, and δ is the "density effect". The density effect, δ, is evaluated by the empirical form given by Sternheimer in References 4 and 5.

Proton Range-Energy Calculation - The proton range is defined as the distance penetrated before coming to rest. For a proton of energy E_o incident on a shield layer of thickness x, CHARGE computes the transmitted energy E_2 and the range corresponding to the transmitted proton energy $R(E_2)$:

$$E_2 = E_o\left(1 - \frac{x}{R_o}\right)^{1/\gamma}$$

$$R(E_2) = R_o\left(\frac{E_2}{E_o}\right)^{\gamma}$$

To accomplish this, an initial estimate of the transmitted energy E_1 is made

$$E_1 = E_o + x \frac{dE_o}{dx}$$

and the approximate energy loss rate dE_1/dx established. Assuming the range-energy relationship to be of the form

$$R(E) = R_o \left(\frac{E}{E_o} \right)^{\gamma}$$

then

$$- \frac{dE}{dx} = \frac{dE}{dR} = \frac{E_o}{\gamma R_o} \left(\frac{E_o}{E} \right)^{\gamma - 1}$$

The values of γ and R_o required to establish E_2 and $R(E_2)$ are obtained by substituting E_o and E_1 in the latter expression and rearranging terms:

$$R_o = - \frac{E_o}{\gamma} \Big/ \frac{dE_o}{dx}$$

$$\gamma = 1 + \frac{\ln(-dE_1/dx) - \ln(-dE_o/dx)}{\ln(E_o/E_1)}$$

Electron Energy Loss Rates - CHARGE uses the average energy loss formula for relativistic electrons, including exchange, spin, density, and quantum mechanical effects, and an approximate correction for energy loss due to bremsstrahlung emission:

$$\frac{dE}{dx} = \frac{4\pi e^4}{mv^2} NB$$

where

$$B = \left\{ \left[\ln \frac{mv^2 E}{2I^2(1-\beta^2)} - \left(2\sqrt{1-\beta^2} - 1+\beta^2\right) \ln 2 + 1-\beta^2 + \frac{1}{8}\left(1 - \sqrt{1-\beta^2}\right)^2 \right] \left(1 + \frac{EZ}{1600mc^2}\right) - \delta \right\}$$

This formula results from combining several equations given by Bethe and Ashkin in Reference 3. At energies below a specified value E_{ce}, dE/dx is held constant, as for protons.

Bremsstrahlung production is of little importance as an energy loss mechanism for electron energies normally encountered, although it is a significant source for dose determinations.

Electron Transmission Calculation - Electron transmission is computed, optionally, by a range-energy method or by semi-analytical transmission factors. The electron range-energy option assumes the same functional relationship between penetration and energy as is used for protons. The semi-analytical transmission factors are derived from Monte Carlo data (Reference 6); the transmission factor treatment is normally used in preference to the range-energy method for shields of a single material. In order to improve results obtained through the use of transmission factors for laminates of various materials, electron penetration studies using an analytic transport code are in progress. The data from these investigations will be incorporated in CHARGE as they become available.

3.1.2 Secondary Radiation Calculations

Secondary radiations treated by CHARGE are electron bremsstrahlung and neutrons and protons from primary proton interactions with shield materials. The transport functions for secondary protons are identical to those for primary protons of the same energy

The secondary particle dose rates are represented by the integral:

$$\dot{D}_\beta(x) = \int_{E_\ell(x)}^{E_h} dE \int_0^{E_h} dE_\beta \int_0^x dx' \phi_\alpha(E) \sum_{\alpha\beta}\left(E'(E,x), E_\beta\right) \exp\left[-\int_0^x \sum_{ne}\left(E'_\alpha(E,x)\right) dx'\right] T_\beta(x-x', E_\beta) R\left(E'_\beta(E_\beta, x-x')\right)$$

where $\sum_{\alpha\beta}\left(E'(E,x), E_\beta\right)$ is the cross section for production of secondary particle type β with energy E_β from primary type α with the energy E_α, (cm^{-1})

$T_\beta(x-x', E_\beta)$ is the transport function for particle type β, created with energy E_β at position x' to the detector at x, (dimensionless)

$R\left(E'_\beta(E_\beta, x-x')\right)$ is the flux to dose rate conversion for particle type β at degraded energy E'_β, $\left(\frac{rad/hr}{Mev/cm^2\text{-}sec}\right)$.

Secondary Nucleons - Cross section data for production of secondary nucleons by nucleons striking complex nuclei have been generated and/or compiled at Douglas, as reported in Reference 7. This treatment separates the product nucleons into a forward-peaked high-energy (cascade) phase and an isotropic low-energy (evaporation) phase. CHARGE incorporates the secondary nucleon production data, as presented in Reference 7, with the single exception that all cascade particles are treated as being emitted straight-ahead; Alsmiller et al have shown this assumption to be valid for all secondary nucleons (Reference 8). In CHARGE, secondary nucleons are calculated for a single characteristic element in each shield material.

Since the low energy protons are much more effective in depositing energy than are high energy protons, this source is treated more accurately. For low energy

secondary protons, the source is computed by numerically integrating the production cross section over each shield region thickness. The energy dependence of the primary protons is treated by assigning an average energy $\bar{E}_i(x')$ over each energy group i. However the variation of $\bar{E}_i(x')$ with penetration depth x' is accurately computed, so that region thicknesses x are not restricted to small values. The secondary source energy $E_k(x')$ is also treated as position-dependent.

For high energy secondary protons, the dependence of both primary and secondary proton energies, $\bar{E}_i(x')$ and $E_k(x')$, on position within the region is not treated. They are considered to be constant over the region thickness x, because of their large range.

The treatment of the spatial distribution of secondary neutron production is similar to that used for high energy secondary protons. Computed values of total dose are insensitive to the detailed treatment of neutron production because of the significantly lesser attenuation of neutrons along the transmission path as compared to protons.

Secondary neutrons are attenuated using an energy-dependent (group-wise) removal cross section for neutron energies greater than 20 Mev. The neutron non-elastic cross section data for this computation are presented in Reference 7. For lower neutron energies, a constant value of the removal cross section, based on the shield material traversed, is applied.

Electron Bremsstrahlung - Several formulations of the bremsstrahlung production cross section are incorporated in CHARGE, providing a means of comparing results from the various techniques for calculating the source of this dose component.

The empirical treatment by Evans (Reference 9) is the simplest model and yields results which agree reasonably well with a combination of Bethe-Heitler non-screened cross sections and various cross sections compiled by Koch and Motz (Reference 10). The photons thus generated are transported from the source point to the detector location by exponential attenuation and buildup. The calculated photon spectra, which are transmitted through the shield, bracket the experimental spectra of Edelsack (Reference 11) for 1.0 to 2.0 Mev electrons.

An experimental program has been initiated by Douglas to determine energy and angular distributions of photons produced by electrons over the energies, and in the materials, applicable to space vehicle shielding.

3.1.3 Dose Rate Calculations

Charged Particles - At each shield region interface, CHARGE computes the dose rate due to incident charged particles, including the effects of absorption and energy loss in the region already traversed. Since the doses are not computed at each mesh interval, the number of regions is determined by the desired number of dose points and the actual number of physically distinct layers, while the number of mesh intervals is determined by error limits on the accuracy of the range-energy integration and computer running time limitations. In general, the mesh intervals should be thinner than ten per cent of the range of the highest energy particles.

To evaluate charged particle contributions to biological dose, CHARGE currently has two options: one of these assumes the "relative biological effectiveness" (RBE) of deposited energy is a function of particle energy, the other assumes RBE is a function of the energy loss rate or linear energy transfer (LET).

Neutrons - For the neutron dose calculation, values of neutron dose per unit flux are input as a function of neutron energy. Up to ten pairs $\left(E, D/\phi(E)\right)$ are input. Power law interpolations to the average energy of each neutron group are performed from the table. The dose is then a product of this factor and the group fluxes, summed over all neutron groups.

Bremsstrahlung - The bremsstrahlung dose rate is computed from the energy flux values using tabulated values of the mass energy absorption coefficients (μ_a/ρ) for the material; RBE is defined as unity for x- and γ-rays. The dose conversion assumes a logarithmic energy relationship to exist between entries in the absorption coefficient table in order to compute group-averaged dose conversion factors; the initial establishment of the group boundaries requires that each group lie between consecutive entries in the μ_a/ρ table.

3.2 Comparative CHARGE Results

Results from CHARGE calculations are presented in Figure 2 through 5; these are typical of comparative results presented in the report on the CHARGE program (Reference 2).

3.2.1 Bremsstrahlung Spectra in Aluminum

In CHARGE, electron bremsstrahlung production may be calculated by the Born approximation or by a simple formula given by Kulenkampf (Reference 12). Figure 2 presents a comparison of bremsstrahlung photon spectra calculated by each of these methods with experimental data of Edelsack et al (Reference 11). These data have been renormalized to represent the photon flux integrated over all solid angles. The spectra are those transmitted through an aluminum slab just thick enough to stop the monoenergetic incident electrons.

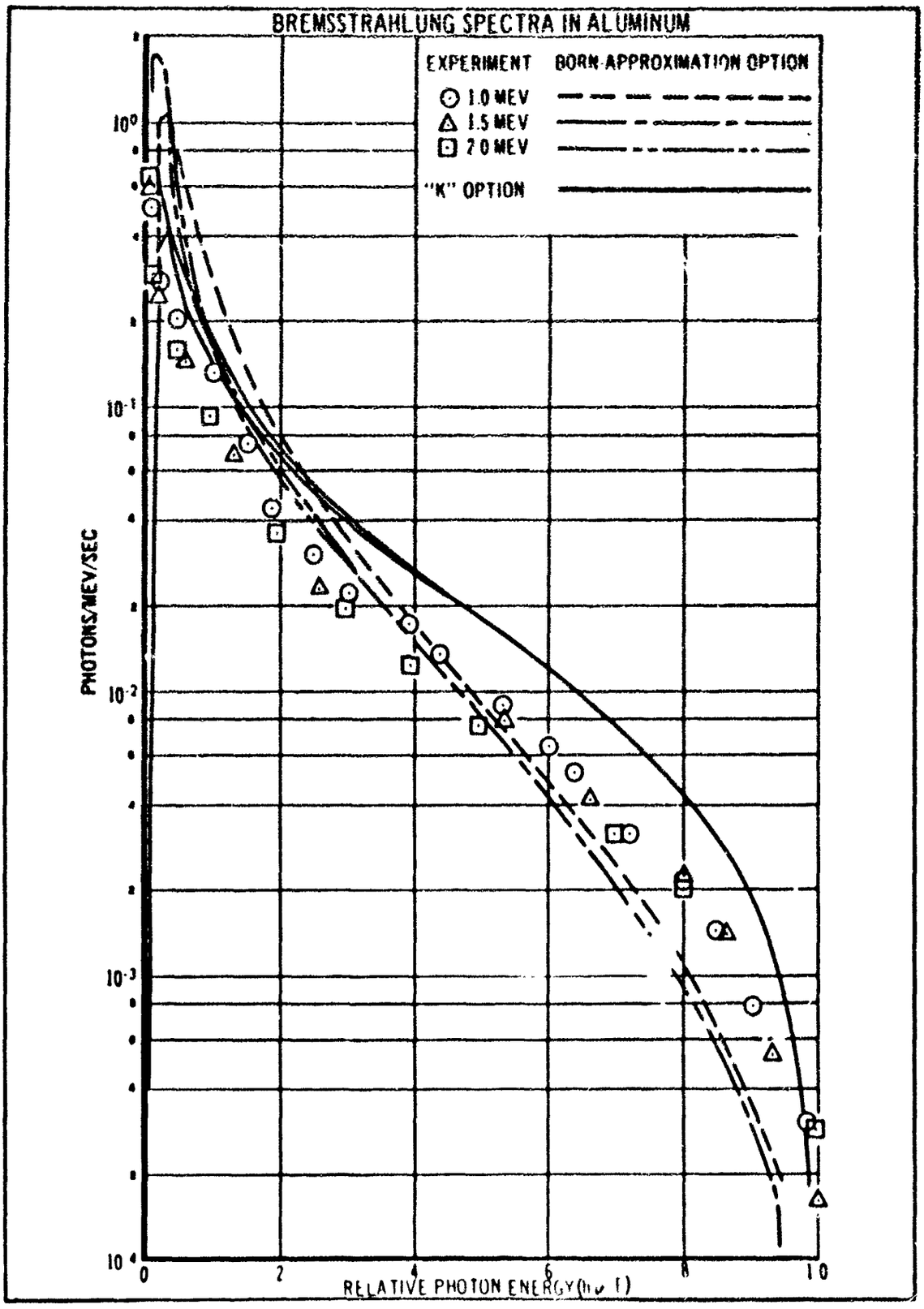
BREMSSTRAHLUNG SPECTRA IN ALUMINUM
EXPERIMENT
BORN APPROXIMATION OPTION
1.0 MEV
1.5 MEV
2.0 MEV
"K" OPTION
PHOTONS/MEV/SEC
RELATIVE PHOTON ENERGY (hν / T)

FIGURE 2

DOSE CALCULATION FOR ARTIFICIAL ELECTRON BELT

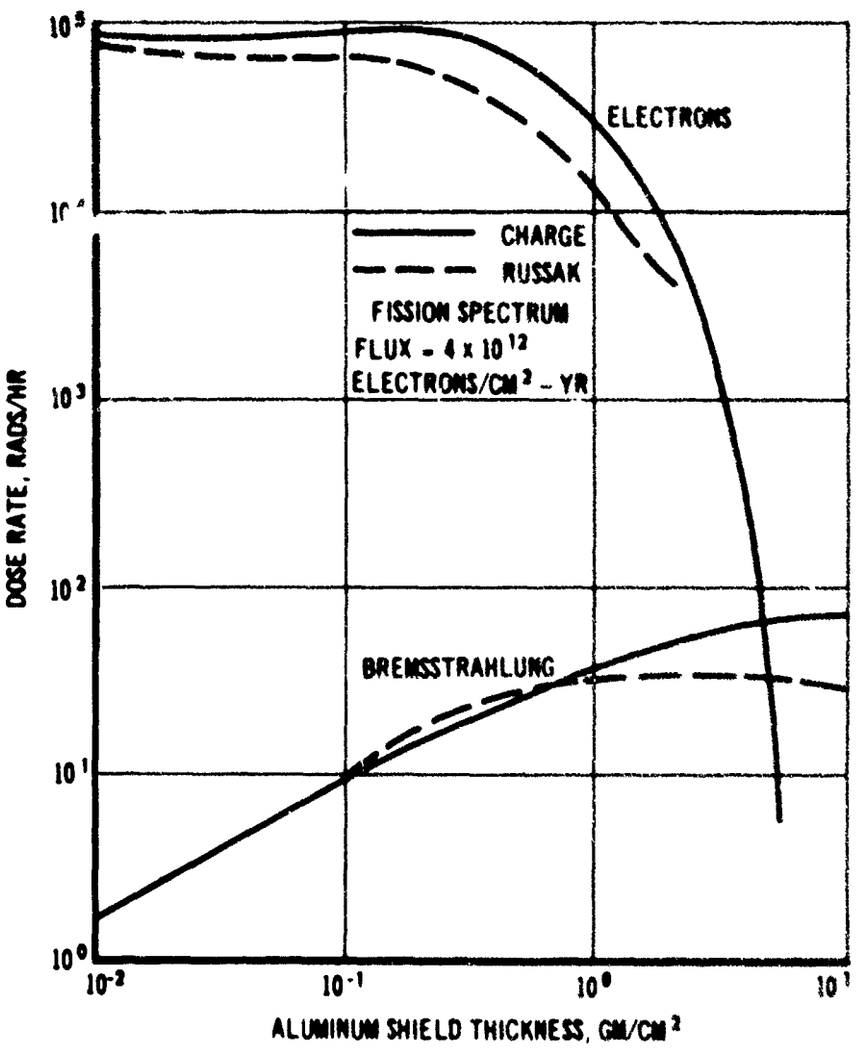

FIGURE 3

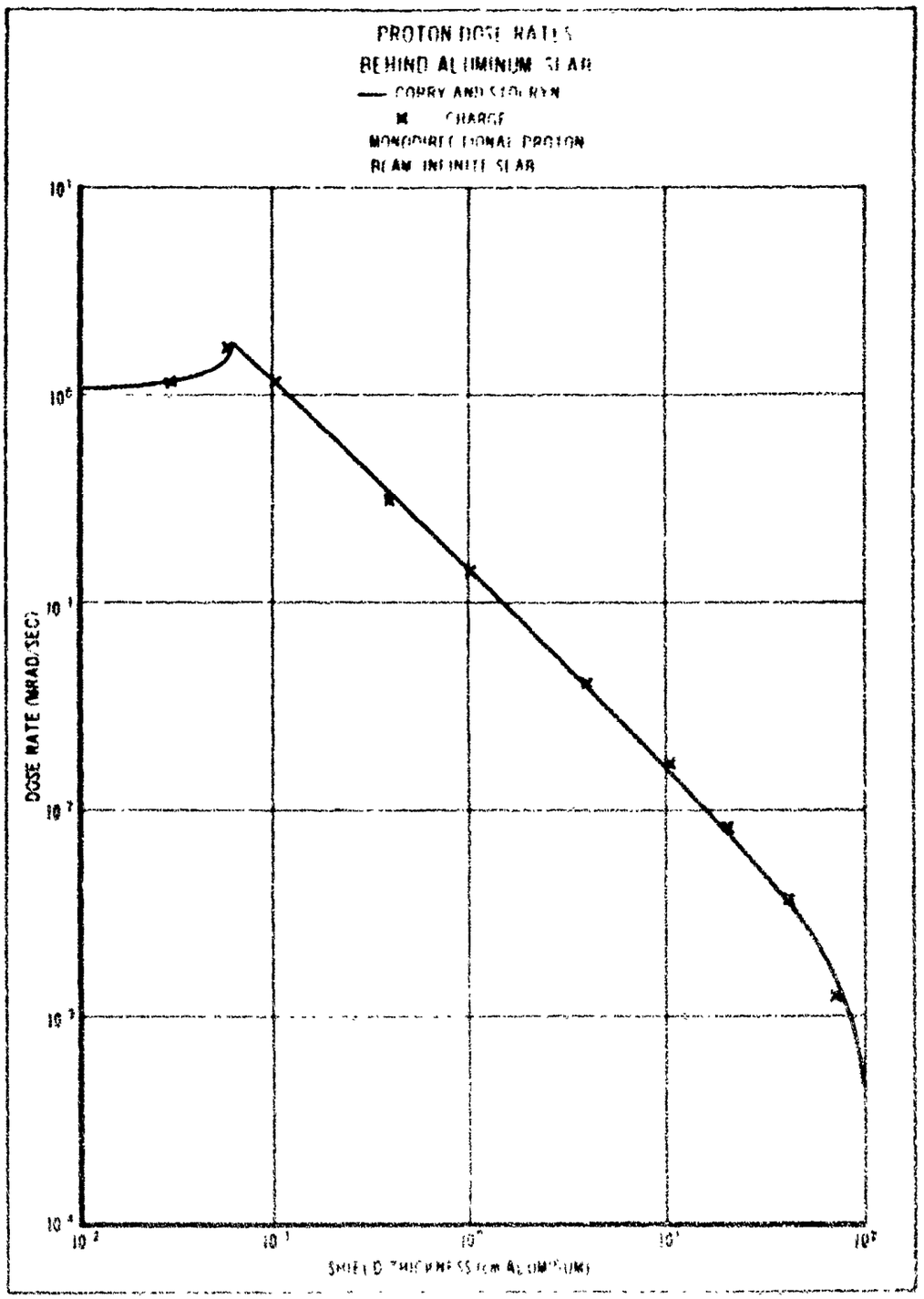
PROTON DOSE RATES
BEHIND ALUMINUM SLAB
— CORRY AND STOLOVY
✖ CHARGE
MONODIRECTIONAL PROTON
BEAM INFINITE SLAB
DOSE RATE (MRAD/SEC)
SHIELD THICKNESS (cm ALUMINUM)

FIGURE 4

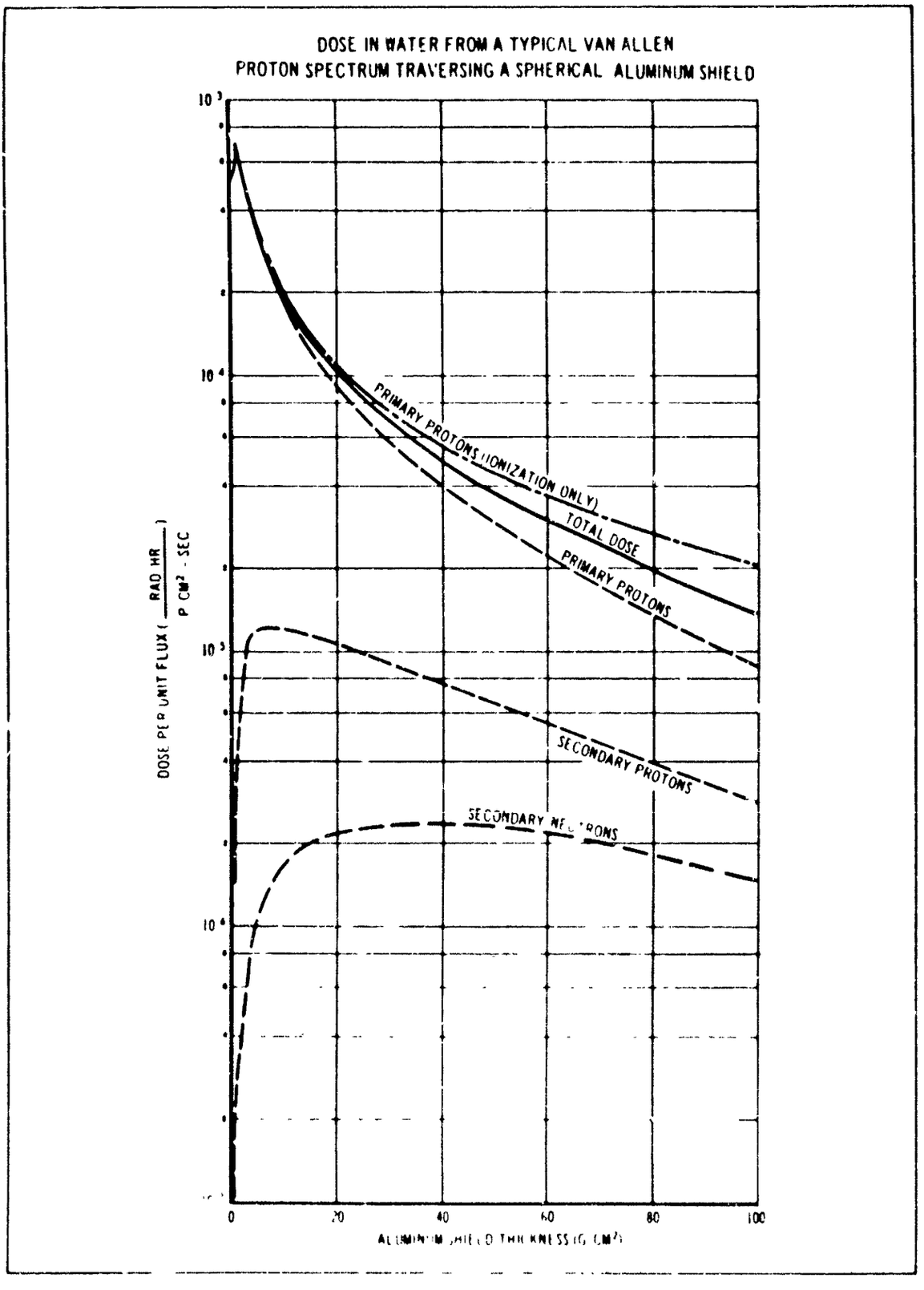
DOSE IN WATER FROM A TYPICAL VAN ALLEN
PROTON SPECTRUM TRAVERSING A SPHERICAL ALUMINUM SHIELD
PRIMARY PROTONS (IONIZATION ONLY)
TOTAL DOSE
PRIMARY PROTONS
SECONDARY PROTONS
SECONDARY NEUTRONS
0
20
40
60
80
100

FIGURE 5

Since the Kulenkampf (or "K") model predicts identical relative spectra for all electron energies, multiple curves appear only where the photon absorption differs. The K option is normally used for shielding analyses because it predicts a spectrum in better agreement with experimental data for a wide range of materials, and because it is a very simple form.

3.2.2 Dose Calculation for Artificial Electron Belt

Dose calculations were performed for an electron spectrum, approximately representing the artificial electron belt, incident on an infinite aluminum shield. The electron transmission calculation used the range-energy option (52 electron groups) rather than the more accurate semi-analytical transmission factor method. The bremsstrahlung source was computed from empirically corrected Born approximation cross sections.

Results are compared with data published by Russak (Reference 13) in Figure 3. The agreement is generally good. Differences in the two electron dose curves may be attributable to the use of different flux-to-dose conversion factors.

These data are indicative of the dose rate which would be received by an astronaut performing operations external to the space vehicle and therefore protected only by a space suit. The dose rate under these conditions is relatively insensitive to the incident electron energy spectrum, since $\frac{dE}{dx}$ is not a strong function of energy over the electron energy range of interest.

3.2.3 Proton Dose Comparison with Analytic Range-Energy Data

Corry and Stogryn calculated the dose behind an aluminum slab exposed to a monodirectional proton flux typical of the Van Allen belt (Reference 14).

The analytic calculation assumed the proton range to be approximated by a single power law of energy for all protons. CHARGE results, obtained using the properly adjusted isotropic ambient flux, are compared with this work in Figure 4. The agreement is excellent.

The cusp of the curve is a direct result of the fact that the incident spectrum was specified only for energies above 10 Mev. As the lowest energy protons slow down, their biological effectiveness increases, this effect predominating until the penetration corresponding to the range of 10 Mev protons is reached (cusp of figure), at which point proton absorption predominates and dose decreases with depth. This type of behavior appears whenever the incident spectrum is unspecified for low energies.

3.2.4 Dose Calculation for Van Allen Protons

A typical Van Allen proton spectrum was represented for two energy ranges by

$$\frac{d\phi}{dE} \sim E^{-0.72} \qquad (30<E<80 \text{ Mev})$$

$$\frac{d\phi}{dE} \sim E^{-1.80} \qquad (80<E<700 \text{ Mev})$$

and normalized to a flux of one proton/cm^2-sec. The detailed dose contributions computed by CHARGE for primary protons and secondary protons and neutrons behind an aluminum shield are shown in Figure 5. A comparison is made with results from an ionization calculation which assumes that all energy losses are due to ionization since the attenuation of primary charged particles is governed principally by this method. For this proton spectrum, the ionization method, which requires much less computer time, yields a good approximation to the total dose for small shield thicknesses, but is conservative with increasing shield depth.

3.2.5 Dose Calculation for Solar Flare Protons

In Figure 6, the dose received from a solar flare of the November 12, 1960 type is presented as a function of aluminum shield thickness. The differential proton spectrum was approximated in three energy regions by

$$\frac{d\phi}{dE} = 1.77 \times 10^{13} E^{-3} \qquad (30 < E < 80 \text{ Mev})$$

$$\frac{d\phi}{dE} = 9.62 \times 10^{16} E^{-5} \qquad (80 < E < 440 \text{ Mev})$$

$$\frac{d\phi}{dE} = 6.63 \times 10^{18} E^{-5.4} \qquad (440 < E < 6600 \text{ Mev})$$

which corresponds to an integrated flux of 9.04×10^{9} protons/cm^2. The ionization calculation gives doses within ten per cent of the detailed calculation for shield thicknesses less than 30 g/cm^2. For shield thicknesses greater than about 30 g/cm^2, the dose from secondary radiation is important because of the rapid attenuation of the primary proton dose. This behavior is characteristic of the steep primary proton spectra typically associated with solar flare events.

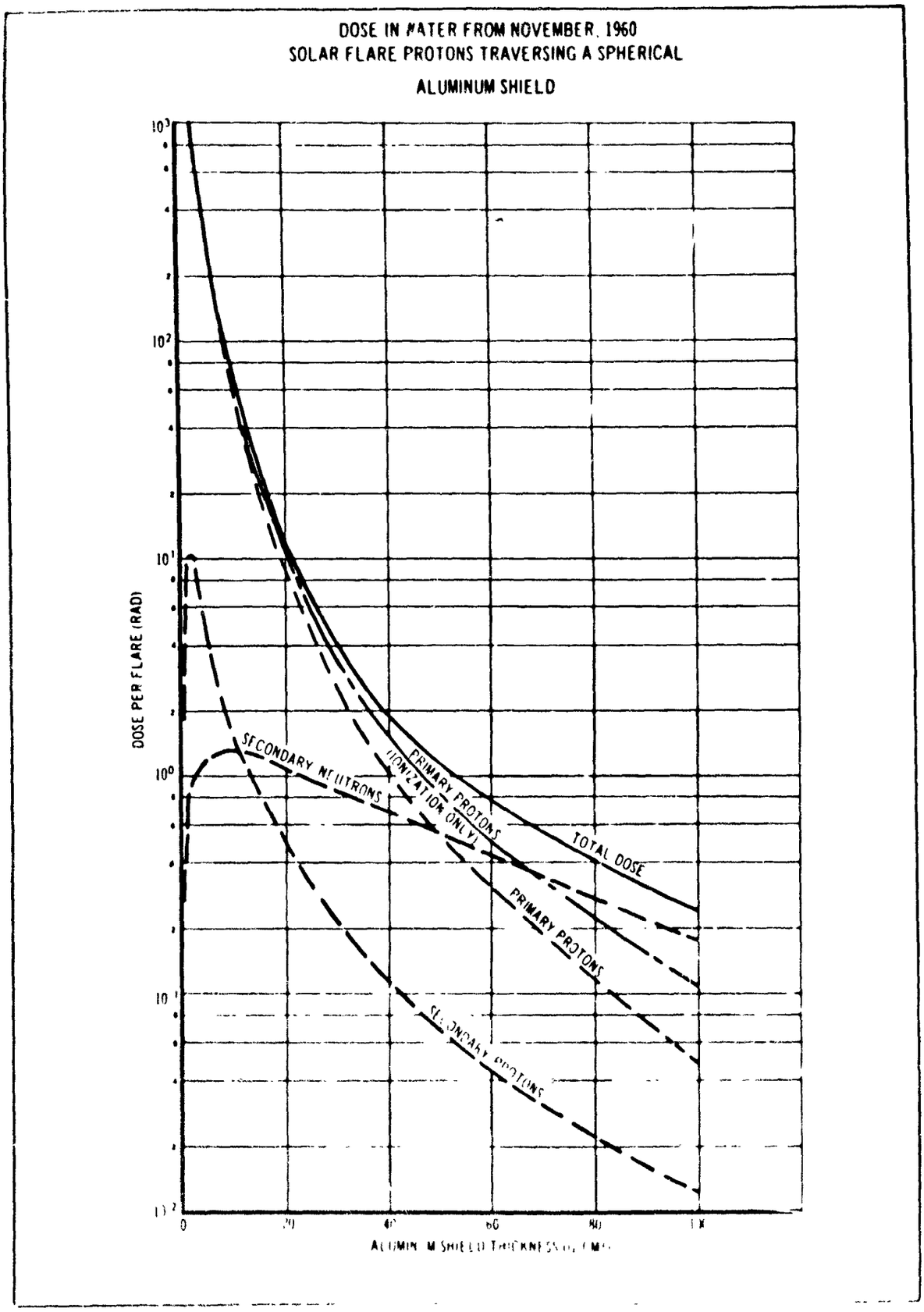
DOSE IN WATER FROM NOVEMBER, 1960
SOLAR FLARE PROTONS TRAVERSING A SPHERICAL
ALUMINUM SHIELD
DOSE PER FLARE (RAD)
SECONDARY NEUTRONS
PRIMARY PROTONS
(IONIZATION ONLY)
TOTAL DOSE
PRIMARY PROTONS
SECONDARY PROTONS

FIGURE 6

4.0 APPLIED SHIELDING

The evaluation of shielding requirements for a space vehicle system necessitates a detailed treatment of the actual system geometry. Dose computations are often extremely sensitive to inhomogeneities in the spatial distribution of structural and shield materials, equipment and stores, etc., so that an accurate description of the material distribution is essential. Since the shielding physics calculations of radiation - materials interactions are restricted to simple geometries, these methods are normally applied to construct kernel functions which can then be used for dose evaluations by applying ray tracing procedures to complex geometric systems. At Douglas, the geometric description of a realistic space vehicle is performed by the SIGMA program, which incorporates a numerical procedure for angular integration of dose attenuation kernels constructed by the CHARGE program. Geometric operations within SIGMA are performed using the QUAD generalized quadric surface geometry package.

It can be important to consider carefully the geometric distribution of biological materials about the critical, radiation-sensitive body organs of crew members. For thinly shielded systems, particularly for extravehicular operations performed in a space suit, the shielding afforded by body tissues may represent the greater part of the total effective shielding. Therefore studies comparing dose computations for various extant man models have been performed. This work has resulted in an improved mathematical model being outlined, which is based on a Cartesian coordinate representation of body material distributions The objective of this work is to provide a standard against which results from simpler models can be measured.

The determination of shield weight requirements for specified vehicles and missions is strongly dependent on the allowable shield geometric framework. The distribution

of shield materials among various locations onboard the vehicle, and the shaping of shield thicknesses over extended areas, can be important when seeking to meet the radiation level design criteria for minimum shield system weight. At present, Douglas is adapting powerful mathematical optimization techniques, previously used in neutron and gamma shielding studies, for application to space radiation shielding optimization investigations.

4.1 Detailed Treatment of Vehicle Geometry

The treatment of actual vehicle-shield geometries in radiation level calculations involves the use of ray-tracing techniques. The geometric description of physical regions, and the determination of path lengths traversed by radiations penetrating the vehicle regions, is accomplished by the QUAD geometry package. The QUAD subroutine is under the control of the SIGMA program which sets up the angular intervals for a numerical integration of dose contributions over the solid angle about each receptor locations, and which controls variations in shield thicknesses, shield materials, etc., for parametric shielding studies.

4.1.1 Geometry Calculations

The Douglas QUAD subroutine is a powerful and efficient method for describing geometric systems by generalized quadric surfaces. The system geometry is described by a set of material regions with one or more boundaries which are defined by equations of the form:

$$A_o + A_1x + A_2y + A_3z + A_4x^2 + A_5y^2 + A_6z^2 + A_7xy + A_8yz + A_9xz = 0$$

where A_o, A_1, ..., A_9 are input constants and (x, y, z) are the usual Cartesian coordinates. The version of this subroutine used with SIGMA allows up to 100 surfaces and 100 regions for system description.

QUAD performs the following functions under the control of the SIGMA program:

1) Input of the system geometry description.

2) Determination of the region occupied by a point with specified coordinates.

3) Determination of the regions traversed, the path length in each region, and the boundary crossed in leaving each region, for a ray specified as to origin and direction.

QUAD incorporates several features which ease input requirements, reduce the possibility of input and calculational errors, and promote computational efficiency. These include the following:

1) The "ambiguity index" is internally computed for each boundary of each region. This index has the value +1 or -1 depending on the location of the region, inside or outside respectively, with respect to the surface forming this boundary.

2) Surfaces are defined separately from the geometric regions to eliminate duplication of data when a surface forms a boundary of more than one region.

3) All distances to surfaces are computed and stored independent of the region boundaries, thus eliminating repetitive calculation of such quantities for those surfaces which bound a number of regions along a specified ray.

4.1. Dose Evaluation

The SIGMA program calculates the dose received at each of a set of specified points internal to a vehicle-shield system by a numerical Simpson's rule

integration of the equation:

$$D(\vec{r}) = \frac{1}{4\pi} \int_{-1}^{1} \int_{0}^{2\pi} K(\vec{r},\vec{\Omega})\,d\Theta\,d\mu$$

where $\vec{r}$ = dose point location

$D(\vec{r})$ = dose received at point $\vec{r}$

μ = the cosine of the polar angle

Θ = the azimuthal angle

$\vec{\Omega} = \sqrt{1-\mu^2}\,(\cos\Theta\vec{i} + \sin\Theta\vec{j}) + \mu\vec{k}$ (a unit vector in the direction defined by μ and Θ)

The number of intervals in the μ and Θ integrations are variable, with systems of pronounced asymmetry requiring a larger number of intervals. The kernel $K(\vec{r},\vec{\Omega})$ represents the dose that would be received at $\vec{r}$ if the material thickness encountered along a ray from $\vec{r}$ in the direction of $\vec{\Omega}$ were spherically symmetric about $\vec{r}$. These material thicknesses are calculated by the Douglas computer subroutine QUAD; the kernel, $K(\vec{r},\vec{\Omega})$ is evaluated for the computed material distribution along the ray from either curve-fit CHARGE data or from a complete CHARGE calculation.

Two options which can be used concurrently are provided for the calculation of the dose received through various outer sections of the vehicle. The first provides a dose breakdown according to specified geometrical regions through which the radiation enters the vehicle, and the second limits the ranges of integration of the angular variables.

integration of the equation:

$$D(\vec{r}) = \frac{1}{4\pi} \int_{-1}^{1} \int_{0}^{2\pi} K(\vec{r},\vec{\Omega})\, d\Theta\, d\mu$$

where $\vec{r}$ = dose point location

$D(\vec{r})$ = dose received at point $\vec{r}$

μ = the cosine of the polar angle

Θ = the azimuthal angle

$\vec{\Omega} = \sqrt{1-\mu^2}\,(\cos\Theta\vec{i} + \sin\Theta\vec{j}) + \mu\vec{k}$ (a unit vector in the direction defined by μ and Θ)

The number of intervals in the μ and Θ integrations are variable, with systems of pronounced asymmetry requiring a larger number of intervals. The kernel $K(\vec{r},\vec{\Omega})$ represents the dose that would be received at $\vec{r}$ if the material thickness encountered along a ray from $\vec{r}$ in the direction of $\vec{\Omega}$ were spherically symmetric about $\vec{r}$. These material thicknesses are calculated by the Douglas computer subroutine QUAD; the kernel, $K(\vec{r},\vec{\Omega})$ is evaluated for the computed material distribution along the ray from either curve-fit CHARGE data or from a complete CHARGE calculation.

Two options which can be used concurrently are provided for the calculation of the dose received through various outer sections of the vehicle. The first provides a dose breakdown according to specified geometrical regions through which the radiation enters the vehicle, and the second limits the ranges of integration of the angular variables.

Program SIGMA incorporates several features to facilitate parametric studies. Among these are the following:

1) Multiple orbits are treated simultaneously during the geometric calculations. Each orbit may entail several radiation sources and the dose received from each primary and secondary radiation component is printed out.

2) Multiple material sets are allowed, and as a result, each material region can have several different densities; this allows a determination of the variable shielding effects of equipment, supplies, etc., and facilitates parametric studies of shield thickness where geometric effects are negligible and changes in shield thickness can be approximated by changes in material density.

3) The capability to input multiple material sets permits dose attenuation data for various shield materials to be approximated by expressing material thickness in terms of an equivalent density of the base material. This approximation is acceptable for proton, electron, and x-ray or gamma ray doses when the materials are not very dissimilar and the attenuation is not too great. For large parametric studies, it has been found that this can save a great deal of computer time without appreciably affecting the accuracy of the results.

4) Multiple material sets and multiple orbit sets are all treated during a single angular integration, so that geometric computations are not repeated unnecessarily.

5) Dose transmission may be calculated by several alternate methods including a basic transport calculation for the material distribution along each ray traced. For example, a complete CHARGE calculation

can be performed for each ray traced. These calculations can include the effects of anisotropic source distributions.

6) CHARGE data for kernel evaluations are input in tabular form and curve-fitted internally by exponentials or power laws over each interval. This considerably simplifies the preparation of input data over methods which require the determination of coefficients for the kernels external to the program. Anisotropic sources can be treated.

7) Computed dose data for various dose receptor locations in the vehicle can be time-weighted according to prospective work-rest cycles and summed to provide representative total dose data for an entire mission. Such data are obtainable as a function of shield thickness when the option to use successive sets of material data for each shield region is exercised.

8) SIGMA output data on computed dose as a function of such parameters and variables as shield thickness, orbital altitude, orbit inclination, etc., can be plotted directly on an S-C 4020 high speed microfilm recorder operating as peripheral equipment on the Douglas IBM 7094 computer. Considerable flexibility in arrangement and labeling of output data is possible.

4.2 Related Geometric Considerations

In addition to the detailed treatment of vehicle geometry, there exist other considerations of a geometric nature which can be important in establishing shielding requirements for a given space vehicle and mission. One such consideration is the geometric representation of astronauts, particularly the spatial distribution of biological materials shielding critical body organs.

Another is the establishment of the geometric framework within which shield materials are positioned: i.e., the determination of an optimal distribution of shield mass is subject to the number and type of variables defining the potential geometric locations of the attenuating materials.

4.2.1 Dosimetric Anatomical Model of Man

A significant factor in space-radiation analysis is the shielding worth of body tissues enclosing the radiation-sensitive body organs. Thus, one of the important models in computer programs designated for analyzing space-radiation shielding requirements is an anatomical model of man. Several radiobiological man models of varying sophistication have been reported in the space-radiation literature. Some of these models are decided over-simplifications of the human anatomy and of critical organ locations; other models treat the spatial distribution of body materials in considerable detail. Most of the extant man models are deficient in combining accuracy in the representation of body tissue distributions, for a variety of potential body positions, with efficiency in computer application of the model and in preparation of the anatomical input data requisite to its use.

Comparison of computed dose results for two of the commonly applied man models, positioned within a realistic space vehicle, are shown in Figure 7 and 8. Fixed vehicle structure and equipment are worth approximately 2.2 g/cm^2. The "average tissue depth" model assumed 0.3 cm of tissue shielding over a 2π solid angle and infinite shielding over the remainder. The elliptical cylinder model is comprised of two elliptical regions, one representing the head and neck, and other the trunk: cylinders were dimensioned according to mean dimensions of USAF flying personnel (Reference 15). Calculations based on this model are for a dose point 0.3 cm below the surface of the smaller cylinder, at eye level

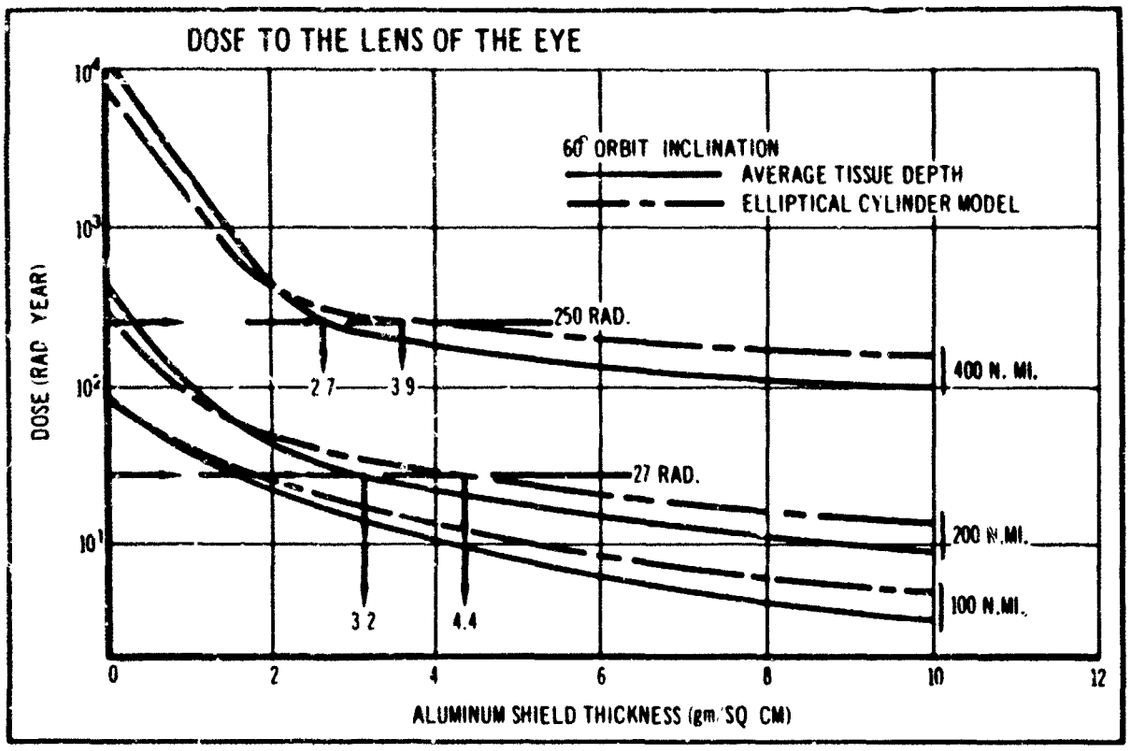

FIGURE 7

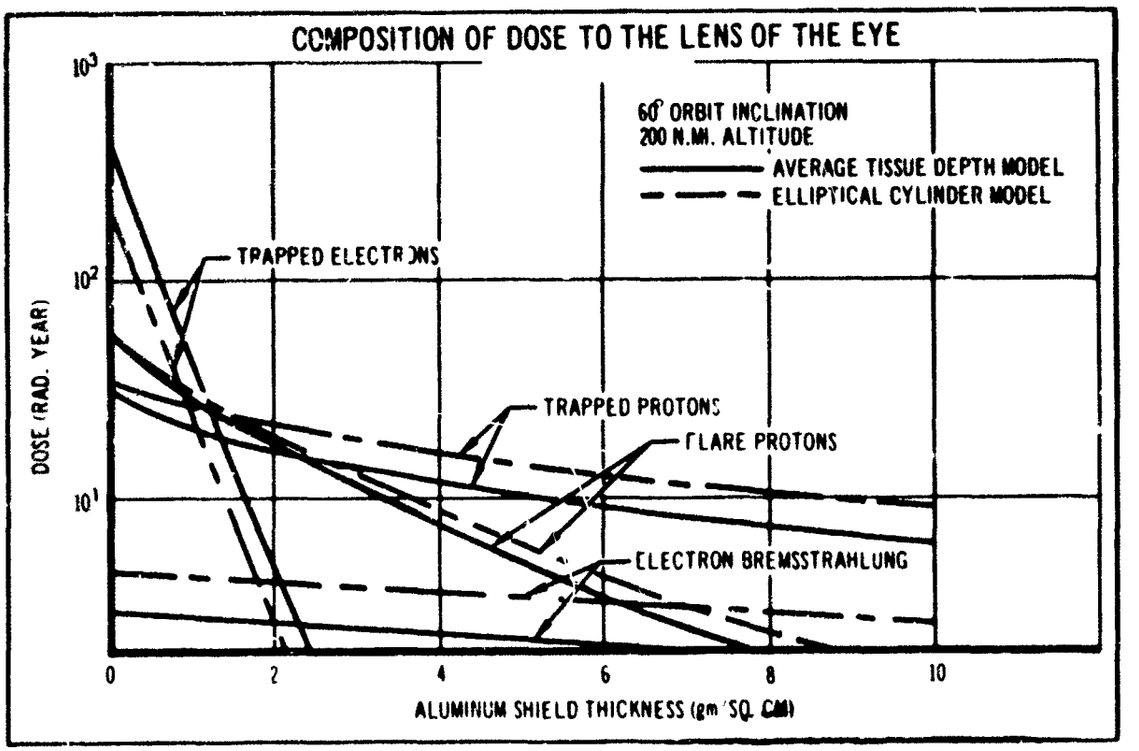

FIGURE 8

Differences between computed dose results for the two models are a direct result of the assumption of 2π infinite shielding for the average tissue depth model. For the readily attenuated trapped electron dose contribution, this assumption results in an over-estimation; i.e., the shielding effect is actually greater than 2π because, in the elliptical model, the slant path along rays deviating significantly from the normal is greater than the average tissue depth of 0.3 cm. For the more penetrating protons and electron bremsstrahlung, the assumptions of 2π infinite shielding results in an under-estimation of dose. This is because the shielding offered by the head is not effectively infinite, as it is for electrons. Comparable results were obtained for dose to the skin and to blood-forming organs.

In the comparison shown, the elliptical cylinder model was taken to be the standard; results based on this model are considered "correct." However, the actual correct values are not known without resort to either empirical data or still more sophisticated mathematical models. Shield weight requirements are quite sensitive to the man model used, as indicated by the pairs of shield thicknesses shown for each of the two design dose criteria: uniformly distributed shielding weighs 3500 lb per g/cm^2 for the reference configuration. Therefore, Douglas has proposed the development of a more sophisticated computerized man model capable of being incorporated into comprehensive programs for dose calculations within realistic vehicle configurations (i.e., SIGMA). Such a model would provide an analytical reference against which dose computations based on other, simpler models could be measured. Preliminary analyses have indicated the development of a Cartesian coordinate model to be attractive. In this approach, the human body is represented as a number of separate regions, i.e., head and neck, torso, upper arm, forearm, etc., each region being characterized

by a rectangular solid geometry. Superimposed on each region is a Cartesian coordinate grid structure defining an array of grid elements, each with a specified average material composition. Advantages of such a model relative to extant man models include:

1) A geometric framework for which grid element composition data may easily be prepared from anatomical cross section drawings.
2) An acceptable approximation to the spatial distribution of body tissues for any body position, by rotation and/or translation of the several separate regions with respect to one another.
3) A geometric framework providing for efficient computation of material distributions and path length segments along rays traversing the grid elements of body regions.

4.2.2 Shield Mass Spatial Distribution

Douglas has investigated procedures for optimization of shield systems associated with nuclear reactor sources on board space vehicles over the past two years. This work has encompassed the development of mathematical optimization techniques, the identification of shield system geometric variables, the specification of multiple radiation level design criteria, and the automatic computation of radiation levels and the derivatives of radiation levels with respect to the specified variables. These investigations have culminated in a series of shield system optimization programs designated "PATCH" after the optimization procedure employed. The PATCH technique has used the characteristic thickness of designated shield regions as variables and has used the various radiation level design criteria to constrain the values of these thicknesses during the optimization operations. The mathematical optimization is based on the formulation of the constraining relationships in a particular manner which promotes an efficient iterative solution of the Lagrange multiplier representation of the design problem.

The extension of these optimization investigations to include space radiation sources and crew compartment shielding geometric variables is now in progress. The current work is directed toward the identification of a flexible framework of variables and constraints such that a great variety of space vehicle configurations can be treated. Therefore, the initial emphasis is on use of parametric dose data from SIGMA computations to establish functional relationships between dose values and shield thickness variables, as required for optimization operations. Completion of this initial phase of the shield optimization investigations will serve to define the essential features of a single comprehensive computer program for performing dose computations in generalized quadric geometry and for optimizing the shield mass distribution subject to the dose design criteria.

Specific consideration is now being given to influencing factors such as:

1) Crew compartment internal arrangement, especially the location of bunks, consoles, rest areas, biowell, etc.
2) Placement of equipment and stores within the crew compartment.
3) Division of shield material among such potential locations as crew compartment wall structure, biowell, and localized and personal portable shields.
4) Shield shaping over extended shield material areas, such as wall structure.
5) Time dependence of dose receptor locations, as influenced by crew work-rest cycles.

An additional aspect of this work is a preliminary treatment of uncertainties in the shielding analysis. This phase is limited to the translation of assumed uncertainties in the intensity of the incident space radiation sources into

uncertainties either in the dose for a fixed shield design, or in the shield design (particularly weight) for specific dose design criteria.

4.3 Results from SIGMA Computations

Computed dose data for various manned orbiting space station configurations have been prepared using the OGRE, CHARGE, and SIGMA computer programs. The dependence of dose values on such parameters as shield thickness, orbit altitude, orbit inclination, and shield material has been published in References 16 and 17.

An example of these dose data is presented here for the typical orbiting space vehicle depicted in Figure 9. For this analysis, doses to the lens of the eye, to the skin, and to the blood-forming organs were computed for an astronaut located in the center of the laboratory area. The man model used in the calculation was comprised of two elliptical cylinders, as discussed in Section 4.2.1. Typical results for dose to the lens of the eye are illustrated in Figure 10.

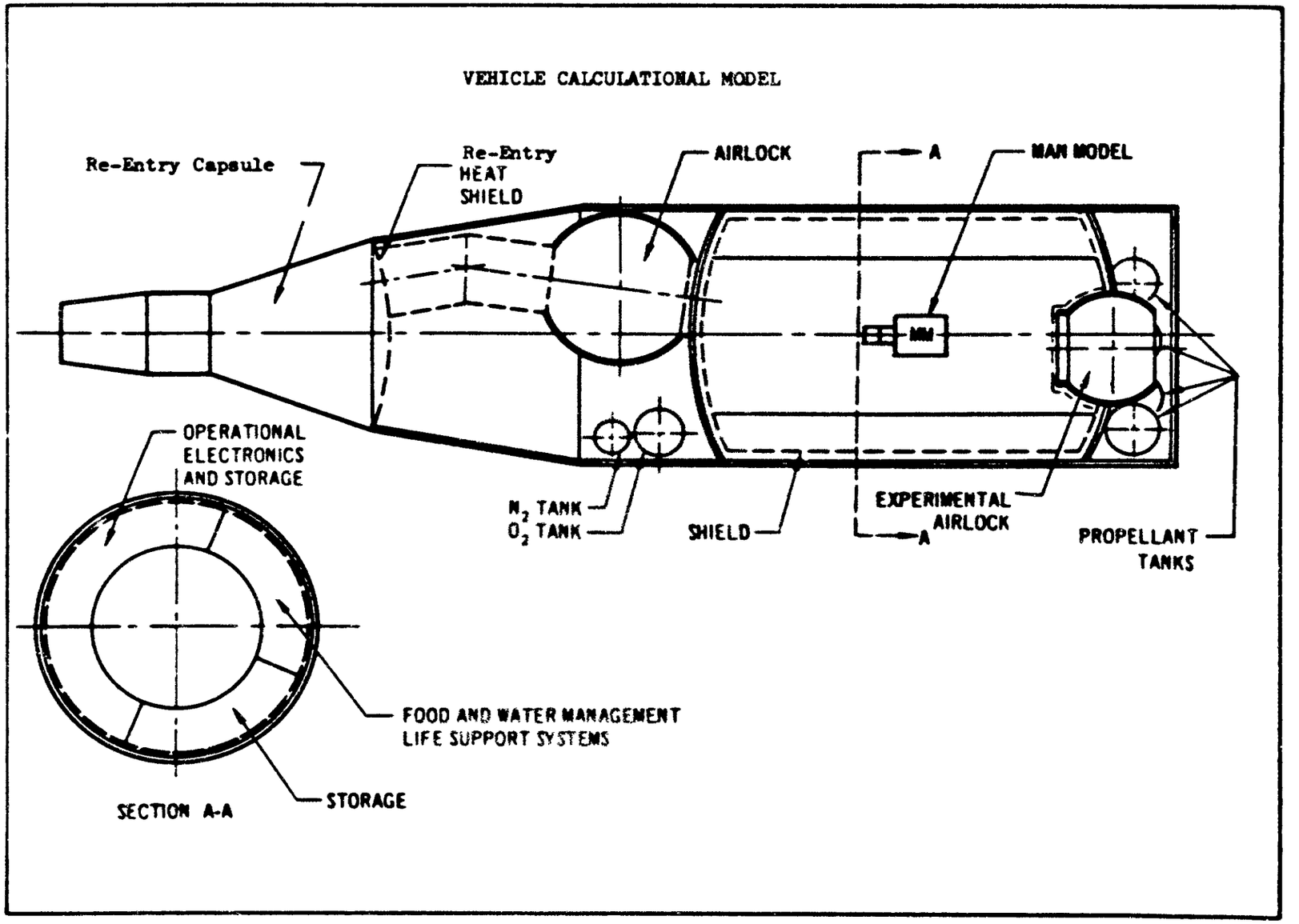
VEHICLE CALCULATIONAL MODEL
Re-Entry Capsule
Re-Entry HEAT SHIELD
AIRLOCK
A
MAN MODEL
MM
OPERATIONAL ELECTRONICS AND STORAGE
N_2 TANK
O_2 TANK
SHIELD
EXPERIMENTAL AIRLOCK
A
PROPELLANT TANKS
FOOD AND WATER MANAGEMENT LIFE SUPPORT SYSTEMS
STORAGE
SECTION A-A

FIGURE 9

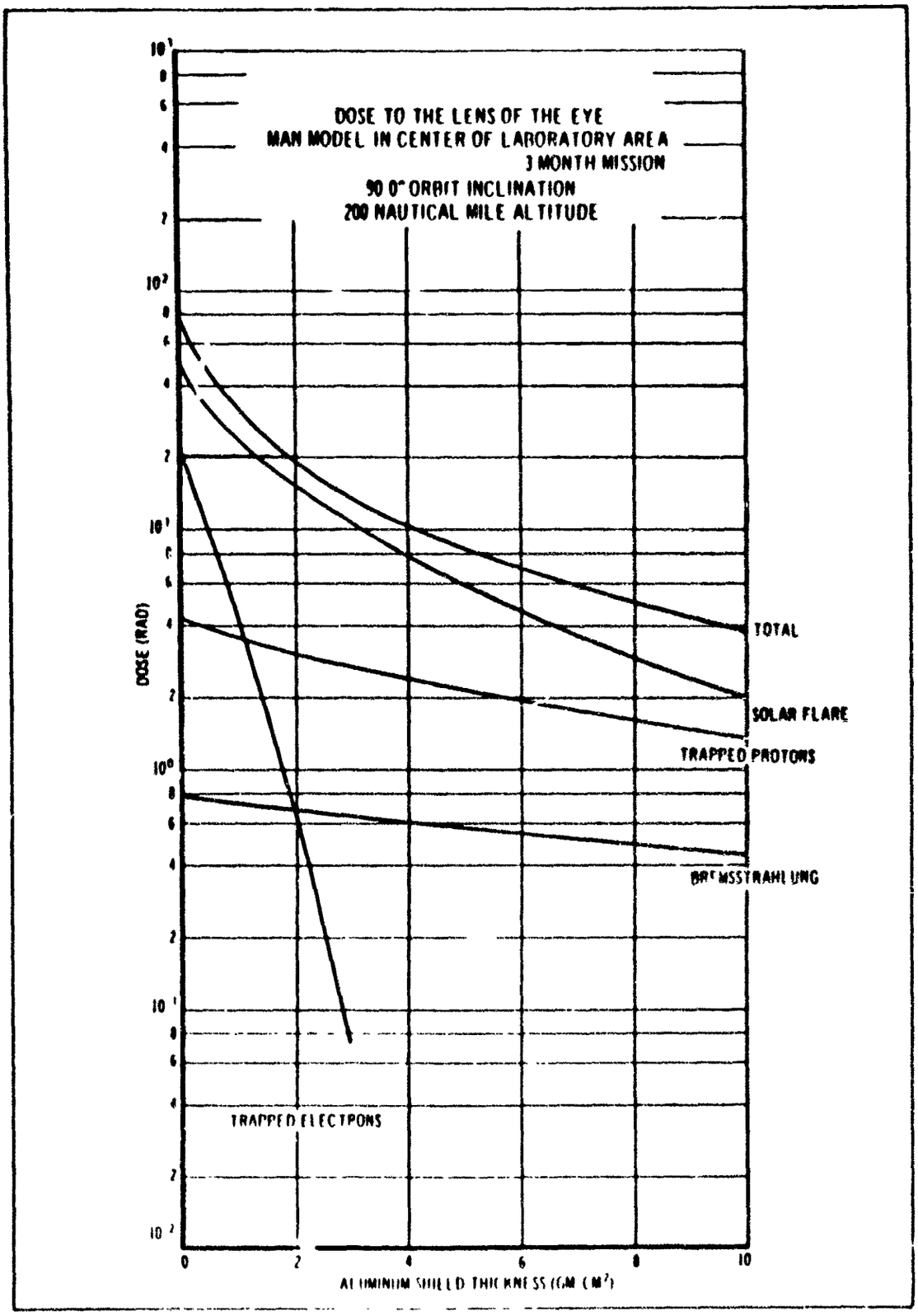
DOSE TO THE LENS OF THE EYE
MAN MODEL IN CENTER OF LABORATORY AREA
3 MONTH MISSION
90.0° ORBIT INCLINATION
200 NAUTICAL MILE ALTITUDE
DOSE (RAD)
TOTAL
SOLAR FLARE
TRAPPED PROTONS
BREMSSTRAHLUNG
TRAPPED ELECTRONS
0
2
4
6
8
10
ALUMINUM SHIELD THICKNESS (GM CM²)

FIGURE 10

REFERENCES

1. Baker, M. B., Geomagnetically Trapped Radiation, Douglas Report SM-47635, dated September 1964.
2. Lilley, J. R., and W. R. Yucker, CHARGE, A Space Radiation Shielding Code, Douglas Report SM-46335.
3. H. A. Bethe and J. Ashkin, "Passage of Radiation Through Matter, in Experimental Nuclear Physics Volume I, E. Segre editor. Wiley, New York City (1953).
4. R. M. Sternheimer, "Density Effect for the Ionization Loss in Various Materials," Phys. Rev. 103, 511 (1956).
5. R. M. Sternheimer, "Range-Energy Relations for Protons in Be, C, Al, Cu, Pb, and Air," Phys. Rev. 115, 137 (1959).
6. Computer Codes for Space Radiation Environment and Shielding, WL TDR-64-71, Vol. I, Air Force Weapons Laboratory, Kirtland AFB, New Mexico.
7. Yucker, W. R., Secondary Nucleons Produced in High Energy Nuclear Reactions, Douglas Report SM-46334.
8. R. G. Alsmiller, Jr., D. C. Irving, W. E. Kinney, and H. S. Moran, The Validity of the Straight Ahead Approximation in Space Vehicle Shielding Studies, paper presented at the Second Symposium on Protection Against Radiations in Space, Gatlinburg, Tennessee, October 1964.
9. Robley D. Evans, The Atomic Nucleus, McGraw-Hill, New York City (1955).
10. H. W. Koch and J. W. Motz, "Bremsstrahlung Cross-Section Formulas and Related Data," Rev. Mod. Phys. 31, 920 (1959).
11. E. A. Edelsack, W. E. Kreger, W. Mallet, N. E. Scofield, "Experimental Investigation of Thick Target Bremsstrahlung Radiation from Electrons of 1.0, 1.5, and 2.0 Mev," Health Physics 4, 1-15 (1960).
12. H. Kulenkampf and L. Schmidt, Ann. Physics, Lpz (5th Series) 43, 494 (1943).
13. S. L. Russak, "Radiation Shielding Considerations in Manned Spacecraft Design," J. Spacecraft 1, 310 (1964).

14. J. E. Corry and D. E. Stogryn, Primary Dose Rate in Slab and Spherical Absorber Systems due to Ionization and Nuclear Attenuation Processes, Lockheed Report LR-16968 (1963).

15. R. E. Fortney, Computer Analysis of Radiation Shielding, AMD-TDR-63-84 (1964), prepared by Northrop Space Laboratories for Aerospace Medical Division, Wright-Patterson AFB, Ohio.

16. T. M. Jordan, E. F. Koprowski and R. W. Langley, Radiation Protection for Manned Orbiting Space Stations, Douglas Report SM-46257.

17. T. M. Jordan, E. F. Koprowski and R. W. Langley, Shielding Requirements for Manned Orbiting Space Stations, Douglas Engineering Paper 3133, presented at the Second Symposium on Protection against Radiations in Space. Gatlinburg, Tennessee, October 1964.